Journal of Alloys and Compounds 505 (2010) 217–223

Contents lists available at ScienceDirect

Journal of Alloys and Compounds

journal homepage: www.elsevier.com/locate/jallcom

Thermodynamic calculation on the stability of $(Fe,Mn)_3AlC$ carbide in high aluminum steels

Kwang-Geun Chin[a,b], Hyuk-Joong Lee[c], Jai-Hyun Kwak[a], Jung-Yoon Kang[b], Byeong-Joo Lee[c,*]

[a] Automotive Steel Products Research Group, POSCO Technical Research Laboratories, POSCO, Jeonnam 545-090, Republic of Korea
[b] School of Materials Science and Engineering, Pusan National University, Pusan, 609-735, Republic of Korea
[c] Department of Materials Science and Engineering, Pohang University of Science and Technology (POSTECH), Pohang 790-784, Republic of Korea

ARTICLE INFO

Article history:
Received 23 February 2010
Received in revised form 7 June 2010
Accepted 10 June 2010
Available online 17 June 2010

Keywords:
Thermodynamic calculation
High Al steel
Phase stability
κ carbide

ABSTRACT

A CALPHAD type thermodynamic description for the Fe–Mn–Al–C quaternary system has been constructed by combining a newly assessed Mn–Al–C ternary description and a partly modified Fe–Al–C description to an existing thermodynamic database for steels. A special attention was paid to reproduce experimentally reported phase stability of κ carbide in high Al and high Mn steels. This paper demonstrates that the proposed thermodynamic description makes it possible to predict phase equilibria in corresponding alloys with a practically acceptable accuracy. The applicability of the thermodynamic calculation is also demonstrated for the interpretation of microstructural and constitutional evolution during industrial processes for high Al steels.

1. Introduction

High aluminum steels (Fe–Mn–Al–C) which have been regarded as a substitution for chromium–nickel stainless steels, are now attracting renewed industrial interest because of their lightweight [1]. Numerous researches have been reported on their deformation or mechanical behavior [2–5], microstructure or transformation behavior [6–9] and also on fundamental materials properties such as stacking fault energy that affect their deformation behavior [10,11]. This class of steels is characterized by the formation of cubic carbide which is referred to as κ, with the Strukturbericht $E2_1$. The κ carbide has a Fe_3Al type $L1_2$ ordered structure with a carbon atom in the central octahedral site, and it can be designated by a formula Fe_3AlC in the Fe–Al–C system. The effect of the κ carbide on the mechanical properties of high Al steels is not clearly known yet. However, once precipitated, the amount is expected to be significant since the composition is rather close to the Fe-rich matrix phase.

For an elaborate control of materials properties, it is essential to understand the microstructural and constitutional evolution. For this purpose, experimental studies on phase equilibria have been performed for the Fe–Al–C [12] and Fe–Mn–Al–C [13] systems. In addition to experimental studies on phase equilibria, as a means of critically assessing and predicting the phase relations under arbitrary thermodynamic conditions, CALPHAD [14–16] type thermodynamic assessments and calculations have been widely used in materials researches. Such an effort for the Fe–Al–C system has been made first by Ohtani et al. [17]. They reported an optimized thermodynamic parameter set for the Fe–Al–C ternary system based on descriptions of the Fe–C [18], Al–C [19], Fe–Al [20] binary systems and first-principles calculation for the enthalpy of formation of the κ carbide. Phase relations were calculated in a wide range of compositions and temperatures. However, the phase equilibria involving fcc (austenite), bcc (ferrite) solid solutions, graphite and the κ carbide in the Fe-rich region has not been reproduced satisfactorily. A similar attempt has been made by Maugis et al. [21] based on the same binary descriptions but on a new first-principles calculation for the κ carbide. Again, the phase equilibria in the Fe-rich region could not be reproduced well, which indicates that the Fe–Al–C ternary system may not be described well by adjusting only the ternary parameters without modifying the existing descriptions for constituent binary systems. Recently, Connetable et al. [22] have concluded that the Fe–Al binary description should be modified in order to reproduce phase relations in the Fe-rich region of the Fe–Al–C ternary phase diagram in good agreement with experimental information. After a reassessment of the fcc and bcc solid solution phases in the Fe–Al system and also after some modifications on metastable parts of the Al–C binary descriptions, they have reproduced phase relations in the Fe-rich region of the Fe–Al–C phase diagram satisfactorily.

* Corresponding author. Fax: +82 54 279 2399.
E-mail address: calphad@postech.ac.kr (B.-J. Lee).

0925-8388/$ – see front matter © 2010 Elsevier B.V. All rights reserved.
doi:10.1016/j.jallcom.2010.06.032

Since practical high aluminum steels include a large amount of manganese, it is necessary to extend the thermodynamic assessment into the Fe–Mn–Al–C quaternary system, which is not available yet especially for the stability of the κ carbide. Based on the successful thermodynamic description of the Fe–Al–C system and existing thermodynamic database for Fe-based alloy systems (for example, TCFE2000 [23] or more recent TCFE5 [24]), the present study constructed a thermodynamic description for the Fe–Mn–Al–C quaternary system. Since thermodynamic descriptions for the Fe–Mn–Al and Fe–Mn–C ternary systems are already available in the database, it is necessary to add those for the Fe–Al–C and Mn–Al–C systems to the database. The thermodynamic description for the Fe–Al–C system was taken from Connetable et al. [22] with some simplifications and the Mn–Al–C system was newly assessed in the present work. Some quaternary parameters were also introduced to better fit experimental information in the quaternary system. The reliability of the finally selected thermodynamic description was evaluated by calculating the stability of the κ carbide in the Fe–Mn–Al–C quaternary alloys and by comparing it with experimental information. The thermodynamic calculation was also used to understand the microstructural evolution in practical high Al steels during industrial processes.

2. Thermodynamic models and assessments

In the CALPHAD method [14–16] the Gibbs energy of individual phases is described using thermodynamic models. Then, the phase equilibria are calculated on the basis of minimum-Gibbs-energy criterion, for example, the Hillert's equilibrium condition [25]. In the original work of Connetable et al. [22] on the Fe–Al–C system, the κ carbide was modeled as an $L1_2$ ordered fcc phase and a special five sublattice model was used. Since this model was connected with the $L1_2$ ordering, information about the effect of Mn on the metastable $L1_2$ ordering in the Fe–Mn–Al system, which is not known and may not be practically important, was necessary to describe the Fe–Mn–Al–C quaternary system. For the sake of simplicity and practical efficiency, in the present work, the κ carbide was modeled using a simpler model as will be described later on. Correspondingly, the fcc solid solution was regarded as a random solid solution without ordering transformations. The B2 ordering that occurs in the bcc solid solution has been modeled on the basis of the two-sublattice compound energy formalism [26,27], and it has been applied to the Fe–Al [28] and also to the Fe–Mn–Al [29] system. The compound energy formalism was further extended to model the $D0_3$ ordering in the Fe–Al system [30]. Temporarily in the present work, however, since the Al content in high aluminum

Table 1
Thermodynamic parameters for the Fe–Mn–Al–C quaternary system.

Liquid: $(Fe,Mn,Al,C)_1$	
$L^{liq}_{Al,C} = 40861.02 - 33.21138T$	[19]
$L^{liq}_{C,Fe} = -124320 + 28.5T + (y_C - y_{Fe})19300 + (y_C - y_{Fe})^2(49260 - 19T)$	[18]
$L^{liq}_{C,Mn} = -168240 + 35.635T + (y_C - y_{Mn})(-91760 + 50T)$	[35]
$L^{liq}_{Al,Fe} = -91976.5 + 22.1314T + (y_{Al} - y_{Fe})(-5672.58 + 4.8728T) + (y_{Al} - y_{Fe})^2 121.9$	[20]
$L^{liq}_{Al,Mn} = -66174 + 27.0988T + (y_{Al} - y_{Mn})(-7509 + 5.4836T) + (y_{Al} - y_{Mn})^2(-2639)$	[34]
$L^{liq}_{Fe,Mn} = -3950 + 0.489T + (y_{Fe} - y_{Mn})1145$	[40]
$L^{liq}_{Al,C,Fe} = -49000$	[22]
$L^{liq}_{C,Fe,Mn} = -45675y_C - 12379y_{Fe} - 12379y_{Mn}$	[39]
bcc: $(Fe,Mn,Al)_1(C,Va)_3$	
${}^0G^{bcc}_{Al:C} = {}^0G^{fcc}_{Al} + 3{}^0G^{graphite}_{C} + 100000 + 80T$	[22]
$L^{bcc}_{Al:C,Va} = 130000 + 14T$	[22]
$L^{bcc}_{Fe:C,Va} = -190T$	[18]
$L^{bcc}_{Al,Fe:Va} = -122960 + 31.9888T + (y_{Al} - y_{Fe})2945.2$	[20]
${}^0Tc^{bcc}_{Al,Fe:Va} = -437.95 \quad {}^1Tc^{bcc}_{Al,Fe:Va} = -1719.7$	[28]
$L^{bcc}_{Al,Mn:Va} = -120077 + 52.851T + (y_{Al} - y_{Mn})(-40652 + 29.2764T)$	[34]
$L^{bcc}_{Fe,Mn:Va} = -2759 + 1.237T$	[40]
${}^0Tc^{bcc}_{Fe,Mn:Va} = 123$	[40]
$L^{bcc}_{Fe,Mn:C} = 34052 - 23.467T$	[39]
fcc: $(Fe,Mn,Al)_1(C,Va)_1$	
${}^0G^{bcc}_{Al:C} = {}^0G^{fcc}_{Al} + {}^0G^{graphite}_{C} + 81000$	[22]
$L^{fcc}_{Al:C,Va} = -80000 + 8T$	[22]
$L^{fcc}_{Fe:C,Va} = -34671$	[18]
$L^{fcc}_{Mn:C,Va} = -43433$	[35]
$L^{fcc}_{Al,Fe:Va} = -104700 + 30.65T + (y_{Al} - y_{Fe})22600 + (y_{Al} - y_{Fe})^2(29100 - 13T)$	[22]
$L^{fcc}_{Al,Mn:Va} = -69300 + 25T + (y_{Al} - y_{Mn})8800$	[34]
$L^{fcc}_{Fe,Mn:Va} = -7762 + 3.865T + (y_{Fe} - y_{Mn})(-259)$	[40]
${}^0Tc^{fcc}_{Fe,Mn:Va} = -2282 \quad {}^1Tc^{fcc}_{Fe,Mn:Va} = -2068$	[40]
$L^{fcc}_{Al,Fe:C} = -104000 + 80T + (y_{Al} - y_{Fe})81000$	[22]
$L^{fcc}_{Fe,Mn:C} = 34052 - 23.467T$	[39]
$L^{fcc}_{Al,Fe,Mn:Va} = 0$	[41]
$L^{fcc}_{Al,Mn:C,Va} = -50000$	This work
$L^{fcc}_{Al,Fe,Mn:C} = -679200 + 400T$	This work
κ carbide: $(Fe,Mn)_3Al_1(C,Va)_1$	
${}^0G^{\kappa}_{Fe:Al:C} = 3{}^0G^{fcc}_{Fe} + {}^0G^{fcc}_{Al} + {}^0G^{graphite}_{C} - 115000 + 25.2T$	This work
${}^0G^{\kappa}_{Mn:Al:C} = 3{}^0G^{fcc}_{Mn} + {}^0G^{fcc}_{Al} + {}^0G^{graphite}_{C} - 150920 + 40T$	This work
${}^0G^{\kappa}_{Fe:Al:Va} = \overrightarrow{\overleftarrow{\overrightarrow{\overleftarrow{\overrightarrow{\overleftarrow{}}}}}} 3{}^0G^{fcc}_{Fe} + {}^0G^{fcc}_{Al} - 94000 + 17.6T$	This work
${}^0G^{\kappa}_{Mn:Al:Va} \overleftarrow{\overrightarrow{=}} \overrightarrow{\overleftarrow{\overrightarrow{\overleftarrow{\overrightarrow{\overleftarrow{}}}}}} 3{}^0G^{fcc}_{Mn} + {}^0G^{fcc}_{Al}$	This work
$L^{\kappa}_{Fe,Mn:Al:C} = 9600$	This work
$L^{\kappa}_{Fe:Al:C,Va} = 13752 - 24T$	This work

The values refer to one mole of formula units and are given in SI units.

steels currently investigated remains in the disordered solid solution range, the B2 and $D0_3$ ordering part in the thermodynamic description of the bcc phase was not included for the sake of simplicity.

2.1. Thermodynamic models

An ordinary two-sublattice model and one-sublattice model with Redlich–Kister polynomials for the excess energy term were used for the Gibbs energy of fcc or bcc solid solution and liquid phase, respectively.

The κ carbide in the Fe–Al–C ternary system has been modeled [17,22] using formulas that allow intermixing between Fe and Al, and non-stoichiometry in the carbon content. However, the experimental composition range of the κ carbide was unclear and the calculated Al content range was narrow in both literatures. On the other hand, it was clear that the carbon content in the Fe–Al–C system deviates toward the low carbon content region from the stoichiometric composition Fe_3AlC [12] while that in the Mn–Al–C system exactly meets the stoichiometric composition Mn_3AlC [31]. Therefore, in the present study, the κ carbide was modeled using a three-sublattice model, $(Fe,Mn)_3Al_1(C,Va)_1$ that allows intermixing between Fe and Mn atoms on the cube face site and incomplete filling of C atoms in the central octahedral site of the ordered $L1_2$ structure. By this model, the Gibbs energy of the κ carbide for one mole of formula unit, $(Fe,Mn)_3Al_1(C,Va)_1$, is expressed as follows:

$$G_m = y^{I}_{Fe}y^{III}_{C}{}^{0}G_{Fe:Al:C} + y^{I}_{Mn}y^{III}_{C}{}^{0}G_{Mn:Al:C} + y^{I}_{Fe}y^{III}_{Va}{}^{0}G_{Fe:Al:Va} + y^{I}_{Mn}y^{III}_{Va}{}^{0}G_{Mn:Al:Va} + 3RT(y^{I}_{Fe}\ln y^{I}_{Fe} + y^{I}_{Mn}\ln y^{I}_{Mn}) + RT(y^{III}_{C}\ln y^{III}_{C} + y^{III}_{Va}\ln y^{III}_{Va}) + y^{I}_{Fe}y^{I}_{Mn}y^{III}_{C}L_{Fe,Mn:Al:C} + y^{I}_{Fe}y^{I}_{Mn}y^{III}_{Va}L_{Fe,Mn:Al:Va} + y^{I}_{Fe}y^{III}_{C}y^{III}_{Va}L_{Fe:Al:C,Va} + y^{I}_{Mn}y^{III}_{C}y^{III}_{Va}L_{Mn:Al:C,Va}. \quad (2)$$

Here, y^{I} and y^{III} represent site fraction of individual components in the first and third sublattices, respectively. ${}^{0}G_{i:j:k}$ represents the Gibbs energy of a compound where the first, second and third sublattices are completely filled with component i, j and k, respectively. In the L parameters, the comma separates the components interacting on the same sublattice and the colon separates components on different sublattices.

Table 2
Enthalpy of formation of $L1_2$ Fe_3Al, $E2_1$ Fe_3AlC and Mn_3AlC selected in the present study, in comparison with other calculations (in kJ/gram-atom).

Compound	Present study (298.15 K)	Other calculations (0 K)
$L1_2$ Fe_3Al	−17.5	−19.3[a], −19.3[b], −21.4[c], −18.8[d]
$E2_1$ Fe_3AlC	−18.2	−16.0[a], −18.4[c], −21.7[d], −27.9[e]
$E2_1$ Mn_3AlC	−27.3	−20.2[d]

The reference states are bcc Fe, fcc Al, cbcc Mn and graphite C.
[a] Ref. [22], CALPHAD assessment.
[b] Ref. [37], first-principle calculation.
[c] Ref. [38], first-principle calculation.
[d] Ref. [36], first-principle calculation.
[e] Ref. [17], first-principle calculation.

2.2. Thermodynamic assessments

The optimization is performed with a selected set of experimental data. Each piece of information is given a certain weight

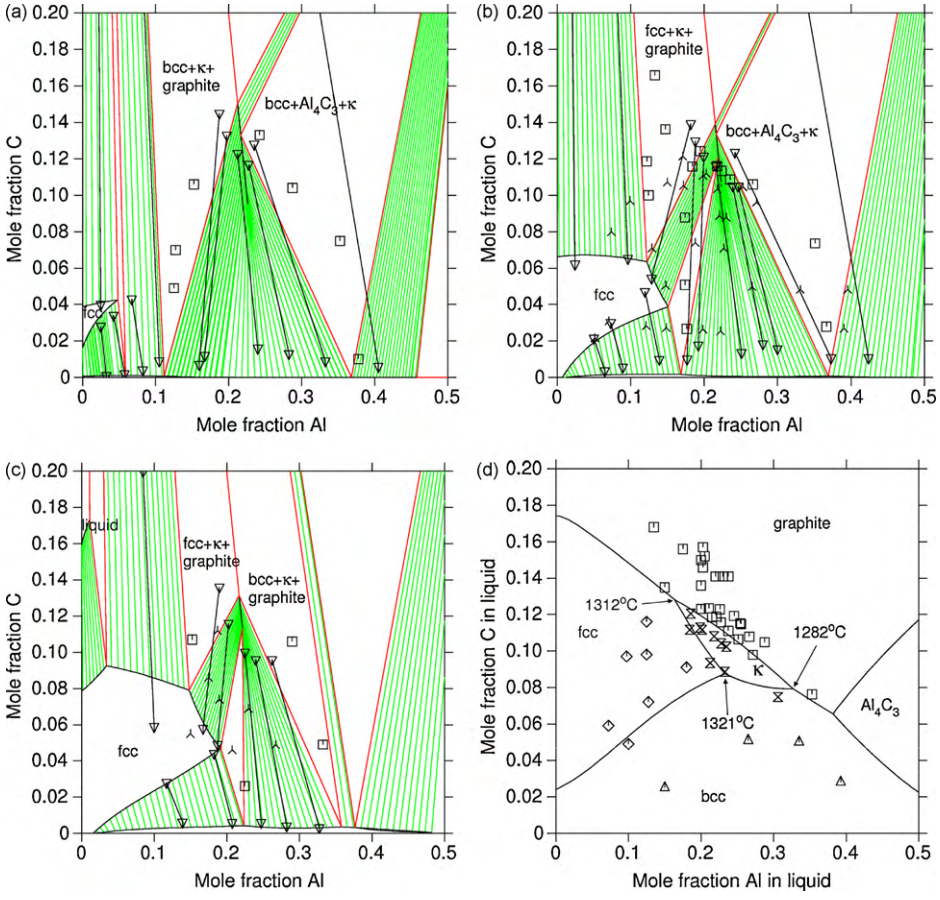

Fig. 1. Calculated isothermal sections at (a) 800 °C, (b) 1000 °C, (c) 1200 °C and (d) liquidus projection of the Fe–Al–C ternary phase diagram, in comparison with experimental information [12].

reflecting the experimental uncertainty. The weight can be changed until most of the selected experimental information is satisfactorily described. All calculations are carried out by using a computer program, Thermo-Calc, developed by Sundman et al. [32].

2.2.1. The Fe–Al–C ternary system

Thermodynamic parameters of only the κ carbide were re-optimized for the Fe–Al–C system, keeping all other parameter values the same as in Ref. [22]. The parameters whose values should be determined were ${}^0G_{Fe:Al:C}$, ${}^0G_{Fe:Al:Va}$ and $L_{Fe:Al:C,Va}$. ${}^0G_{Fe:Al:C}$ and ${}^0G_{Fe:Al:Va}$ correspond to the Gibbs energy of stoichiometric Fe_3AlC and $L1_2$ ordered Fe_3Al, respectively. Even though those compounds do not exist on phase diagrams and no experimental information on their thermodynamic properties is known, first-principles calculations were available for the enthalpy of formation of those compounds. Therefore, the enthalpy of formation values of Fe_3AlC and $L1_2$ ordered Fe_3Al were maintained within the scattering range of first-principles values during the parameter optimization process. Only the entropy of formation of both compounds and the L parameter in a temperature dependent form were optimized by fitting them to the experimental information [12] on the phase relations at 1073 K, 1273 K and 1473 K and liquidus projection. Several equally good parameter sets could be obtained using the first-principles and experimental information for the Fe–Al–C ternary system. After determining the parameters for the Mn–Al–C ternary system, the thermodynamic stability of the κ carbide was calculated for some Fe–Mn–Al–C quaternary compositions. A final adjustment and selection of the above-mentioned parameter sets were made through a comparison with relevant experimental data [33] on the stability of the κ carbide in the quaternary alloys. The result of optimization is presented in the next section in comparison with relevant experimental data.

2.2.2. The Mn–Al–C ternary system

The experimental information on the phase diagram of the Mn–Al–C ternary system was obtained in the form of isothermal sections at 1000 °C and 700 °C through a compilation [31]. Those isothermal sections are characterized by the existence of many three-phase equilibrium triangles. In the present assessment, the Gibbs energy parameters for the Mn_3AlC carbide and Al-rich fcc solid solution were determined so that the constituent phases of individual three-phase equilibrium triangles are correctly reproduced, on the basis of already available thermodynamic descriptions for the Mn–Al [34], Mn–C [35] and Al–C [19] binary systems. As in the Fe–Al–C ternary system, several sets of equally good thermodynamic descriptions were obtained from the information on the Mn–Al–C ternary system because the experimental information on thermodynamic properties of the Mn–Al–C system was not enough to definitely determine the parameter values. The final selection was made by calculating the stability of the κ carbide in the Fe–Mn–Al–C quaternary alloys as has been done for the Fe–Al–C system.

The thermodynamic parameters newly determined in the present study are listed in Table 1. The enthalpy of formation of $L1_2$ Fe_3Al, Fe_3AlC and Mn_3AlC selected in the present study is compared with first-principles values in Table 2.

3. Results and discussion

The calculated isothermal sections and liquidus projection of the Fe–Al–C system are illustrated in Fig. 1. Since only the κ car-

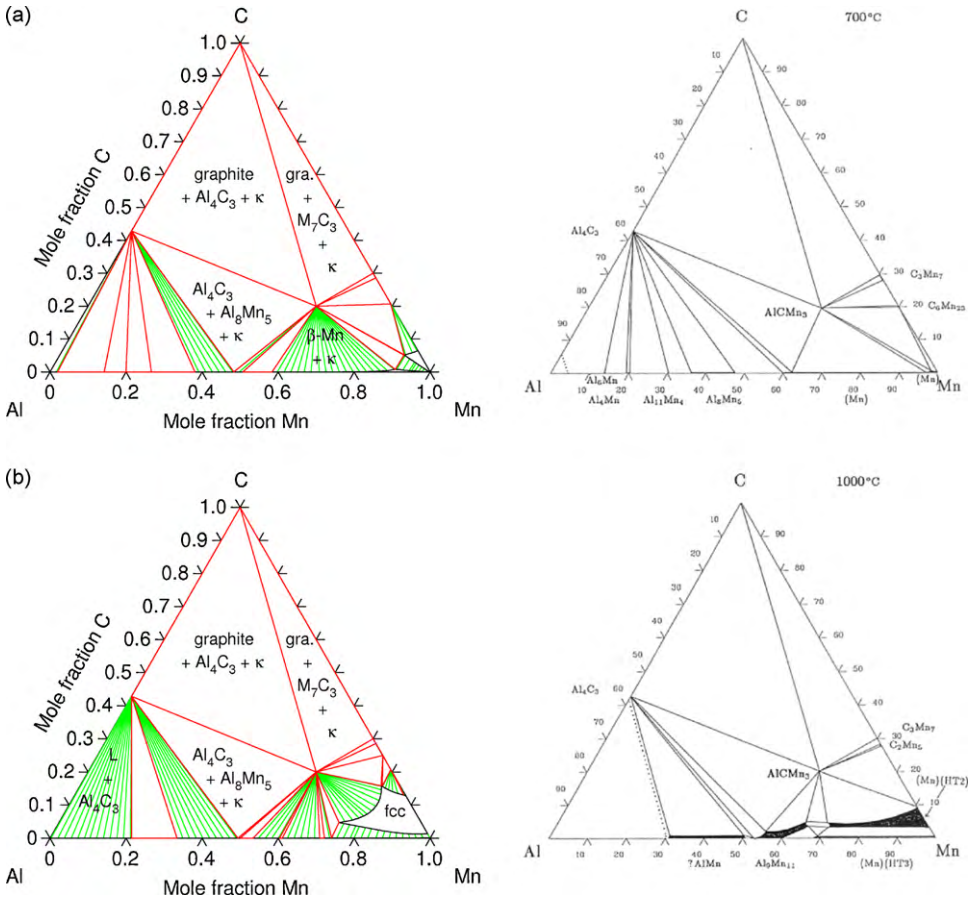

Fig. 2. Calculated and experimentally compiled [31] isothermal sections of the Mn–Al–C ternary phase diagram at (a) 700 °C and (b) 1000 °C.

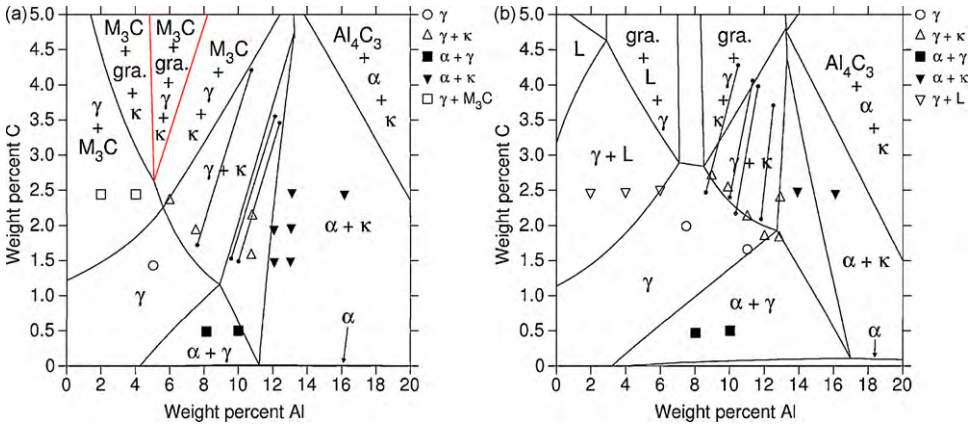

Fig. 3. Calculated phase relations in Fe–20 wt%Mn–Al–C alloys at (a) 900 °C and (b) 1200 °C, in comparison with experimental information [13].

bide is newly modeled and parameterized over the description in Ref. [22], the calculated phase relations are the same as in Ref. [22] except for those related to the κ carbide and the high Al Fe–Al binary side where the B2 ordering is missed. In Fig. 2, the calculated isothermal sections of the Mn–Al–C system are compared with experimental compilations [31]. Efforts were mostly made to estimate a reasonable description for the Gibbs energy of the κ carbide (Mn_3AlC), reproducing the three-phase equilibrium regions. Even with those efforts, some phase relations could not be reproduced exactly by using the present sets of binary descriptions. For example, at 700 °C, the present calculation predicts the existence of a κ/Al_8Mn_5 two-phase equilibrium while the experimental phase diagram shows an Al_4C_3/β-Mn two-phase equilibrium in the compositional range surrounded by κ, Al_4C_3, Al_8Mn_5 and β-Mn. Similar discrepancy between the calculation and experimental data was found also at 1000 °C as shown in Fig. 2b. Furthermore, the finally selected enthalpy of formation of the Mn_3AlC carbide is larger than the recent first-principles calculation as shown in Table 2. All those disagreements were resulted in during the effort to reproduce the stability of κ carbide in the Fe–Mn–Al–C quaternary alloys [33]. Even though the above-mentioned disagreements in the Mn–Al–C ternary system could be improved by adjusting the Mn–Al binary descriptions for intermetallic compounds, we finally decided to wait until such adjustment is needed again in other Mn–Al–metal ternary systems and until more experimental information for the stability of the κ carbide in high Al and high Mn steels is reported.

The upgraded thermodynamic database was used for calculation of phase equilibria in Fe–Mn–Al–C quaternary or more practical higher order alloys. Fig. 3 shows calculated phase relations in Fe–20 wt%Mn–Al–C alloys at 900 °C and 1200 °C, in comparison with experimental information [13]. Even though the agreement is not perfect, the stability of the κ carbide is reproduced fairly well. There was another set of experimental information for the stability of the κ carbide in Fe–30Mn–Al–1C alloys [33]. Fig. 4 shows the temperature and compositional range where the κ carbide precipitates in fcc (austenitic) Fe–30Mn–Al–1C quaternary alloys. The present calculation (solid line) is comparable with experimental information, even though the agreement is not very good, which should be kept in mind in further applications of the present thermodynamic database for higher Al steels. It should be also noted here that according to the present calculation, the bcc solid solution phase (ferrite) appeared as a stable phase in high Al region, while the experiment does not show the formation of bcc phase. Believing that the discrepancy came from a kinetic reason, the calculation for Fig. 4 was performed suspending the bcc phase.

In this work, we have shown that the proposed thermodynamic description for the Fe–Mn–Al–C system enables a prediction of phase equilibria in the corresponding quaternary alloys with a practically acceptable accuracy. We will also demonstrate that the thermodynamic calculation can be used for the interpretation of microstructural evolution in practical multicomponent alloys during an industrial process. Fig. 5a shows microstructures of high Al steels with different alloy compositions. Those steels were annealed at about 1200 °C and hot-rolled, resulting in prolonged grain structures along the rolling direction. In all steels, the microstructure looks as if they are composed of two different areas, the white grey and dark grey regions. The fraction of each area varies depending on the alloy composition. Before a careful TEM work, it is difficult to understand which phases each area represents. However, with thermodynamic calculations for the phase fraction vs. temperature as shown in Fig. 5b, it can be clearly understood that the white and dark grey regions were ferrite and austenite, respectively, at the annealing temperature, and that the ferrite remained while the austenite might have been partially decomposed into ferrite and the κ carbide during the rolling (and cooling). The calculated and experimentally observed phase fractions show a very good correlation indicating that the thermodynamic calculations using the present thermodynamic database can be utilized to estimate the microstructural and constitutional evolution during industrial processes for high Al and high Mn steels.

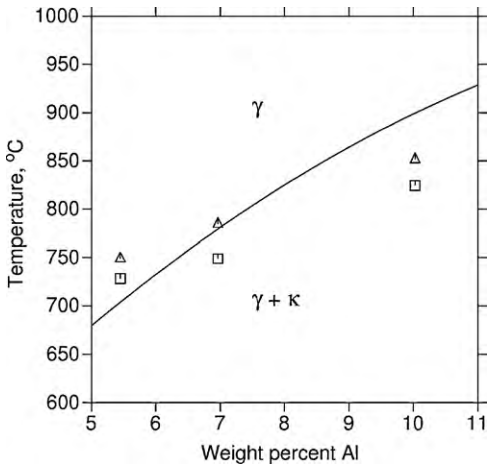

Fig. 4. The effect of Al content on the stability of the κ carbide in Fe–30Mn–Al–1C alloys. The solid line represents the phase boundary by the present calculation and the symbols (squares/triangles) represent phase regions with/without κ carbide from experiment [33].

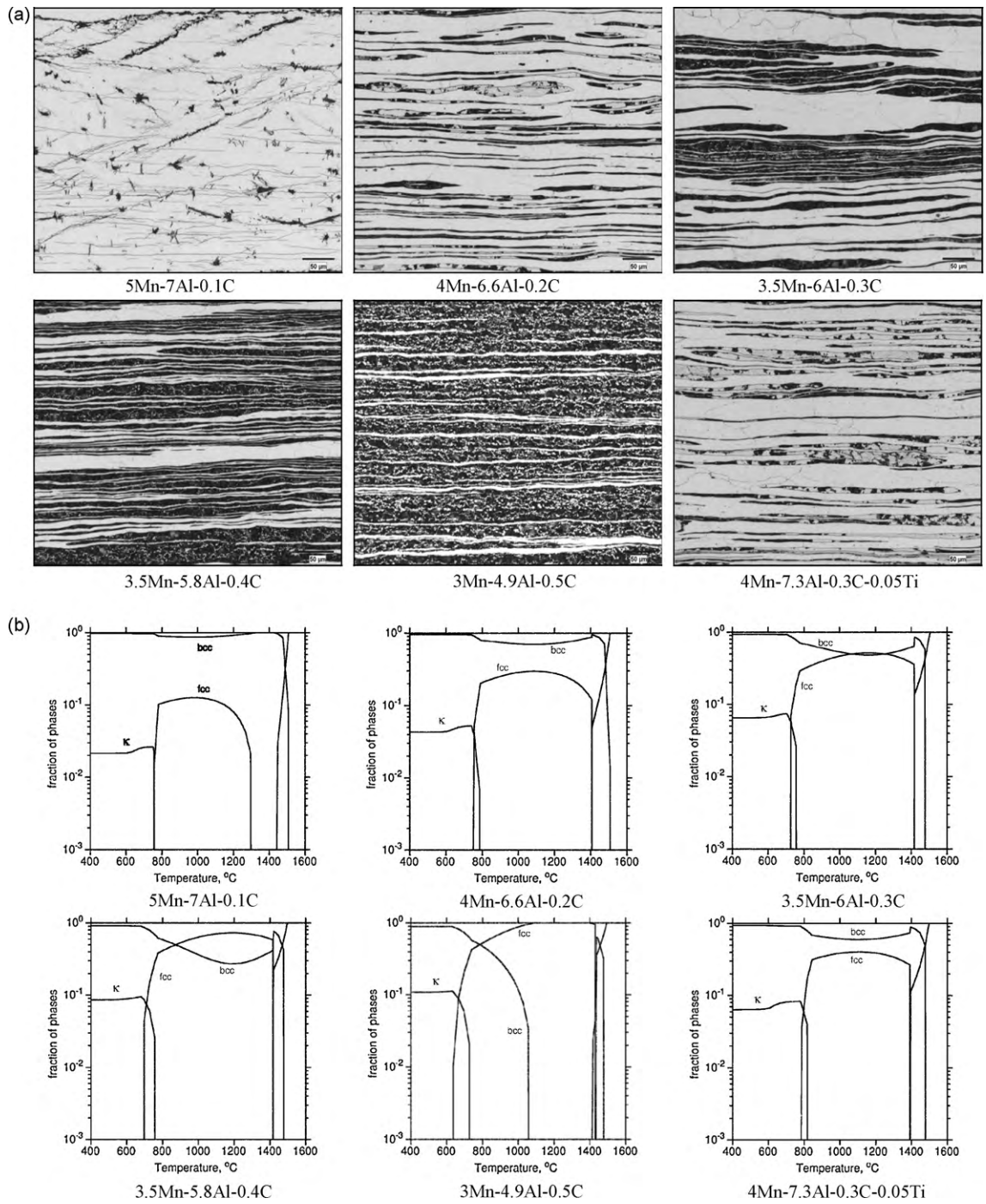

Fig. 5. Comparisons between (a) microstructure of hot-rolled high Al steels and (b) calculated phase fractions (gram-atom fraction) vs. temperature at corresponding compositions.

4. Conclusions

A CALPHAD type thermodynamic description for the Fe–Mn–Al–C quaternary system is made available now, and it can be used for thermodynamic calculations, especially the γ/α phase equilibria and the stability of the κ carbide, in high Al and high Mn steels. The proposed thermodynamic description enables a prediction of phase equilibria in the corresponding alloy systems with a practically acceptable accuracy, and it can also be used for the interpretation of microstructural and constitutional evolution during industrial processes for high Al and high Mn steels.

Acknowledgement

The financial support from POSCO is greatly appreciated (BJL and HJL).

References

[1] G. Frommeyer, U. Brüx, Steel Res. Int. 77 (2006) 627.
[2] J.D. Yoo, S.W. Hwang, K.-T. Park, Metall. Mater. Trans. A 40A (2009) 1520.
[3] J.D. Yoo, S.W. Hwang, K.-T. Park, Mater. Sci. Eng. A 508 (2009) 234.
[4] T. Sahraoui, M. Hadji, M. Yahi, Mater. Sci. Eng. A 523 (2009) 271.
[5] G. Dini, A. Najafizadeh, S.M. Monir-Vaghefi, A. Ebnonnasir, Comput. Mater. Sci. 45 (2009) 959.

[6] D.-W. Suh, S.-J. Park, T.-H. Lee, C.-S. Oh, S.-J. Kim, Metall. Mater. Trans. A 41A (2010) 397.
[7] D. Hua, D. Hao, Z. Xin, T. Zhengyou, Y. Ping, Steel Res. Int. 80 (2009) 623.
[8] B. Bhattacharya, A.S. Sharma, S.S. Hazra, R.K. Ray, Metall. Mater. Trans. A 40A (2009) 1190.
[9] C.-M. Liu, H.-C. Cheng, C.-Y. Chao, K.-L. Ou, J. Alloys Compd. 488 (2009) 52.
[10] K.-T. Park, K.G. Jin, S.H. Han, S.W. Hwang, K. Choi, C.S. Lee, Mater. Sci. Eng. A 527 (2010) 3651.
[11] E. Mazancova, K. Mazanec, Kovove Mater. 47 (2009) 353.
[12] M. Palm, G. Inden, Intermetallics 3 (1995) 443.
[13] K. Ishida, H. Ohtani, N. Satoh, R. Kainuma, T. Nishizawa, ISIJ Int. 30 (1990) 680.
[14] L. Kaufman, H. Bernstein, Computer Calculation of Phase Diagrams with Special Reference to Refractory Metals, Academic Press, New York, 1970.
[15] N. Saunders, A.P. Miodownik, CALPHAD: A Comprehensive Guide, Pergamon Materials series, Elsevier, Oxford, 1998.
[16] H.L. Lukas, S.G. Fries, B. Sundman, Computational Thermodynamics, Cambridge Univ. Press, Cambridge UK, 2007.
[17] H. Ohtani, M. Yamano, M. Hasebe, ISIJ Int. 44 (2004) 1738.
[18] P. Gustafson, Scand. J. Metall. 14 (1985) 259.
[19] J. Gröbner, H.L. Lukas, F. Aldinger, J. Alloys Compd. 220 (1995) 8.
[20] M. Seiersten, SINTEF Report STF-28F93051, Oslo, Norway, 1993.
[21] P. Maugis, J. Lacaze, R. Besson, J. Morillo, Metall. Mater. Trans. A 37A (2006) 3397.
[22] D. Connétable, J. Lacaze, P. Maugis, B. Sundman, CALPHAD 32 (2008) 361.
[23] TCFE2000: The Thermo-Calc Steels Database, upgraded by Byeong-Joo Lee and Bo Sundman at KTH, Stockholm, 1999.
[24] TCFE5 thermodynamic steel database, http://www.thermocalc.se, 2007.
[25] M. Hillert, Physica B 103 (1981) 31.
[26] I. Ansara, N. Dupin, B. Sundman, CALPHAD 21 (1997) 535.
[27] I. Ohnuma, O. Ikeda, R. Kainuma, B. Sundman, K. Ishida, Z. Metallkde. 89 (1998) 847.
[28] I. Ohnuma, Unpublished work, 2000.
[29] R. Umino, X.J. Liu, Y. Sutou, C.P. Wang, I. Ohnuma, R. Kainuma, K. Ishida, J. Phase Equilib. Diff. 27 (2006) 54.
[30] B. Sundman, I. Ohnuma, N. Dupin, U.R. Kattner, S.G. Fries, Acta Mater. 57 (2009) 2896.
[31] P. Villars, A. Prince, H. Okamoto (Eds.), Handbook of Ternary Alloy Phase Diagrams, ASM International, Materials park, OH, 1995, p. 2881.
[32] B. Sundman, B. Jansson, J.-O. Andersson, CALPHAD 9 (1985) 153.
[33] M.C. Li, H. Chang, P.W. Kao, D. Gan, Mater. Chem. Phys. 59 (1999) 96.
[34] A. Jansson, Metall. Trans. A 23A (1992) 2953.
[35] W. Huang, Scand. J. Metall. 19 (1990) 26.
[36] Hanchul Kim, Sookmyung Women's University, Korea, private communication.
[37] F. Lechermann, M. Fähnle, J.M. Sanchez, Intermetallics 13 (2005) 1096.
[38] D. Connétable, P. Maugis, Intermetallics 16 (2008) 345.
[39] W. Huang, Metall. Trans. A 21A (1990) 2115.
[40] W. Huang, CALPHAD 13 (1989) 243.
[41] Bo Sundman, private communication.